A SUBSTRUCTURING APPROACH FOR SIMULATION OF TIME DEPENDENT WORKPIECE DYNAMICS DURING MILLING

CHRISTIAN BRECHER, PRATEEK CHAVAN, ROBERT SPIERLING, MARCEL FEY
Laboratory for Machine Tools and Production Engineering (WZL) of RWTH Aachen University
Aachen, Germany

DOI: 10.17973/MMSJ.2018_12_2018105
e-mail: P.Chavan@wzl.rwth-aachen.de

During milling, the process forces and poor dynamics of the machine may lead to undesirable vibrations between workpiece and tool. The magnitude of these vibrations and the chatter tendency depends mainly upon the dynamic properties of the Tool-Machine-Workpiece system. The dynamic properties of the workpiece can vary significantly during the cutting process, while removing a large volume from a workpiece. Therefore, the aim of this paper is to enable the simulation of time dependent workpiece dynamics by considering its state of material removal.

A method is proposed to incrementally modify the Finite Element (FE) model of the raw workpiecedepending on the volume of removed material obtained by a tool-workpiece penetration simulation, such that an FE model of the intermittent machined state is obtained. This is realized by substructure decoupling in the physical domain. The time-varying dynamic model of the workpiece is thencoupled at four points to spring elementsrepresenting the stiffness of the machine tool table. The developed simulation is subsequently verified by means of vibration measurements and milling tests on a reference workpiece.

KEYWORDS

workpiece dynamics, dynamics substructuring, physical domain, milling

1. INTRODUCTION

During machining, the relative dynamic compliance between the tool cutting edge and the work piece determines the machining accuracy and the stability behavior of the process [Weck 2006]. This relative, oriented FRF (Frequency Response Function) G_g is in turn influenced by several other dynamic compliances such as that of the machine tool structure G_{Struc}, the cutting tool G_{Tool}, the workpiece $G_{Workpiece}$, the workpiece holder, etc. A variation or modification of any of the components, which lie in the force-flux, will result in the change of the system properties, see Figure 1.

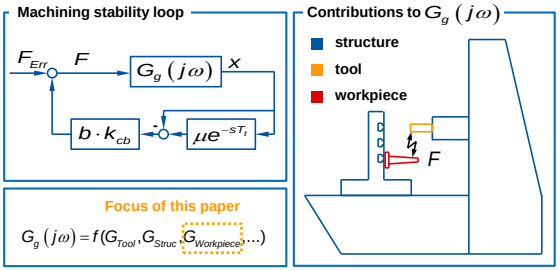

Figure 1. Influences on the dynamic compliance of the system machine tool, work piece and tool, based on [Weck 2006]

With the continuously changing machine position during cutting, the dynamics of the machine structure also varies. This directly influences the relative compliance between tool and workpiece and leads to modification of the process stability boundaries. The simulation of position and hence time dependent dynamics of the machine has been a subject of great interest in the past decade. Yigit and Ulsoy employed a displacement function to describe the change of the dynamic characteristics of the machine tool by assuming the flexible joint interfaces with weak nonlinearity [Yigit 2002]. In [Liu 2011], the authors predicted the variation of modal frequencies of machine tools during working using the matrix perturbation method. In [Liu 2014], a linear dynamic model with variable coefficients was proposed. Two unfixed nodes were created to incorporate the varying configuration of the machine tool and the explicit mass and stiffness matrices with respect to a position were set up.

Apart form the time dependent machine dynamics, the work piece dynamics also plays a significant role in determining the stability behavior. Especially in case of thin walled components with complex geometries like turbine blades and aerospace components.

In [Yang 2016], a method for updating the dynamic model of the workpiece during cutting process is proposed. This is done by performing modal analysis on the FEM model of the initial workpiece, while mode shapes and natural frequencies of the in-process workpiece could be calculated without re-building and re-meshing the instant FEM model at each tool position. Recently, the implementation of substructure models has enabled the efficient prediction of structural

modifications. For example, Law used reduced components models of the machine tool axes in order to estimate the FRFs of the machine for different spatial configurations. This was then used to estimate the modified stability boundaries [Law 2013, Law 2014]. Brecher et al. suggested a method for coupling the reduced matrices of the structural components for any given machine, workpiece and position configuration using multipoint constraints [Brecher 2015, Brecher 2016]. A recent publication by Tuysuz and Altintas [Tuysuz 2017] considers time dependent workpiece dynamics using the dual formulation for frequency based substructure decoupling. The FRFs at the relevant points on the workpiece surface are obtained for different machining states by the recursive decoupling of the dynamics of the material removed. This approach is suitable for thin-walled, flexible workpieces, where the flexibility of the work piece is much higher and the dynamics of the machine can be neglected. However, in cases where the workpiece compliance is comparable to that of the underlying machine structure (workpiece holder, fixture, table, etc.) the machine stiffness cannot be ignored.

In this paper, the influence of time dependent workpiece dynamics is considered by combining a Finite Element discretization, a tool-workpiece penetration simulation and a substructure decoupling approach. The stiffness of the underlying machine structure is considered using spring elements. The aim is to predict the dynamics of the workpiece at different stages of material removal during machining. A substructure decoupling technique is utilized for subtracting the volume of material removed by machining from the FE-model of the unmachined workpiece. For this purpose, a FE-model of a workpiece is created and a method for simulation of tool-workpiece penetration is presented in this paper (Chapter 2). Subsequently, a method is presented for removing the volume of machined material from the model of the unmachined workpiece using substructure decoupling in the physical domain (Chapter 3) Subsequently, the simulated dynamic behavior of a test workpiece at different states of material removal is compared with the measured dynamics of the corresponding physical test workpiece (Chapter 4). Finally, the conclusion and an outlook are presented (Chapter 5).

2. TOOL-WORKPIECE PENETRATION SIMULATION

2.1 Discretization of workpiece

The discretization of the workpiece is crucial for determining the accuracy of the penetration simulation and the computational time. On the one hand, a fine meshallows the accurate representation of the intermediate machining states of the workpiece but on the other hand remains computationally expensive. The factors influencing the mesh size are listed in. The mesh size is dependent on the geometry of the raw part, all intermediate states and onthe final state. For example, a mesh with the edge length of an element as a multiple of the depth of cut, will lead to better results in the penetration simulation. The mesh itself influences the step size of penetration simulation, the discretized tool path and the mesh of the subtraction part. Due to their simple configuration, cubic elements are used for discretization of the workpiece in this paper. Cubic elements with an edge length of 10 mm are chosen here. These elements allow simple rules to determine whether an element is to be considered as penetrated by the tool or not.

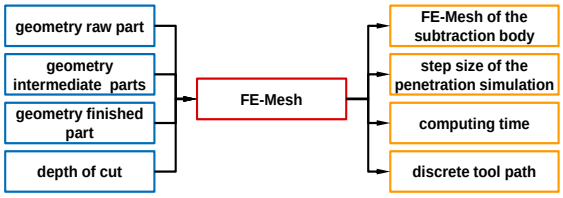

Figure 3. Factors influencing the discretization of workpiece

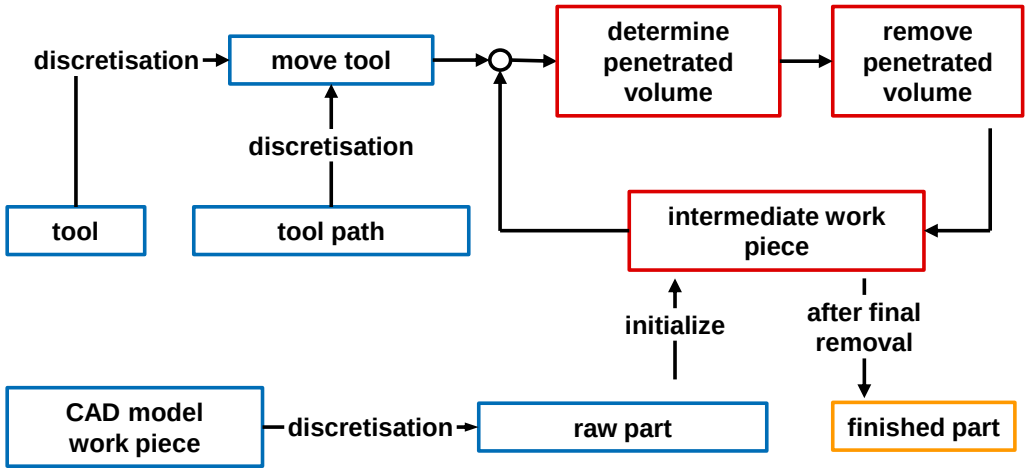

Figure 2. Procedure for tool-workpiece penetration simulation

2.2 Penetration simulation

For a known tool path, cutting parameters and discretized workpiece, discrete intermediate states of the workpiece have to be generated.For this, a tool-work piece simulation is necessary.

Inputs for this simulation are a discrete representation of the workpiece, a discrete tool path and a representation of the milling cutter [Altinas 2014]. The penetration simulation process is illustrated in Figure 2. The material removal process works by identifying theFE elements to be removed and subtracting them repeatedly until an intermediate state of the workpiece is achieved.For this process a method to perform the subtraction of the elements and discretization of work piece, milling cutter and tool path is necessary.

This subtraction of FE is performed by substructure decoupling in the physical domain [De Klerk 2008] and is described further in Chapter 3. Before decoupling the elements, a decision has to be made for every finite element whether it needs to be removed or not. In addition, the physical properties of the element that has to be removed must be known before performing the subtraction. Since cubic elements are used to discretize the workpiece, a single cubic element withhomogeneous material properties serves as a unit for subtraction.

The tool, a milling cutter head of Ø50 mm with four inserts, is represented in the penetration simulation as a cylinder. The tool path is represented by discrete points

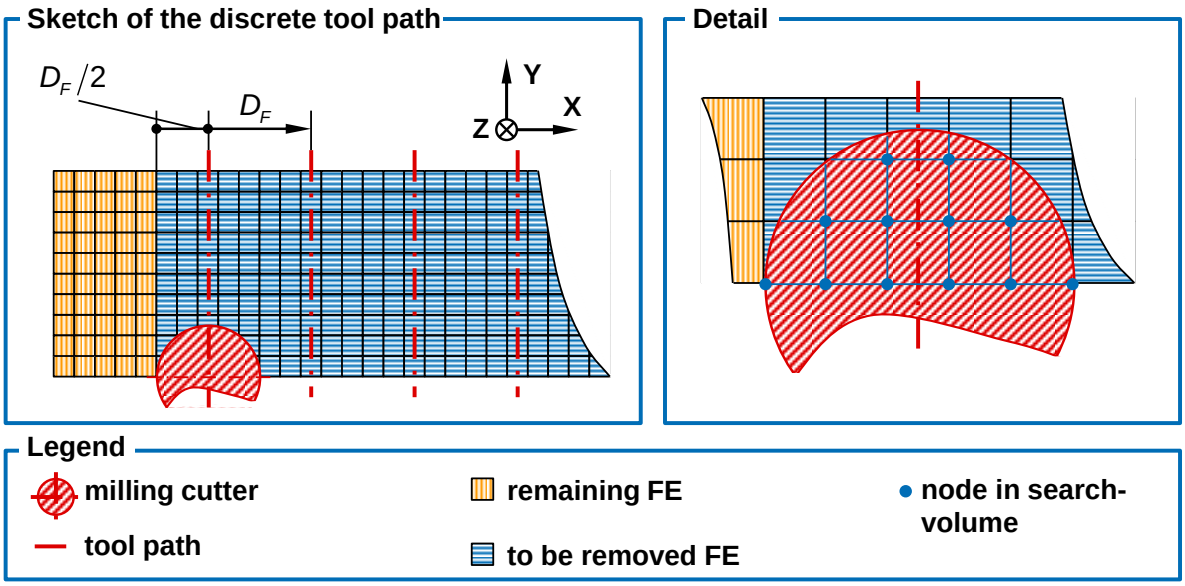

Figure 4. Discretization of tool path and milling cutter

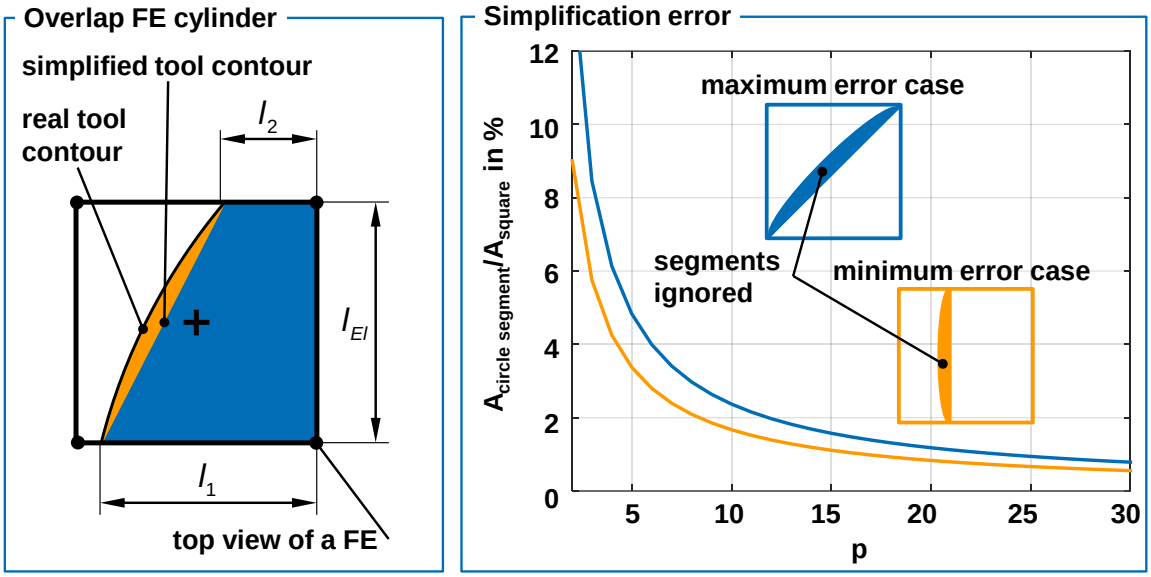

Figure 5. Partly penetration of a FE (top view) and error of the simplification

that have a distance of one FE edge length and are located on the edges of FE, (Fig. 4 right). The milling cutter and an example of tool path discretization can be seen in Figure 4. Here D_F refers to the diameter of the tool.

For the penetration simulation, the workpiece, discretized by cubic elements is used as a basis for a spatial partition representation using volume elements

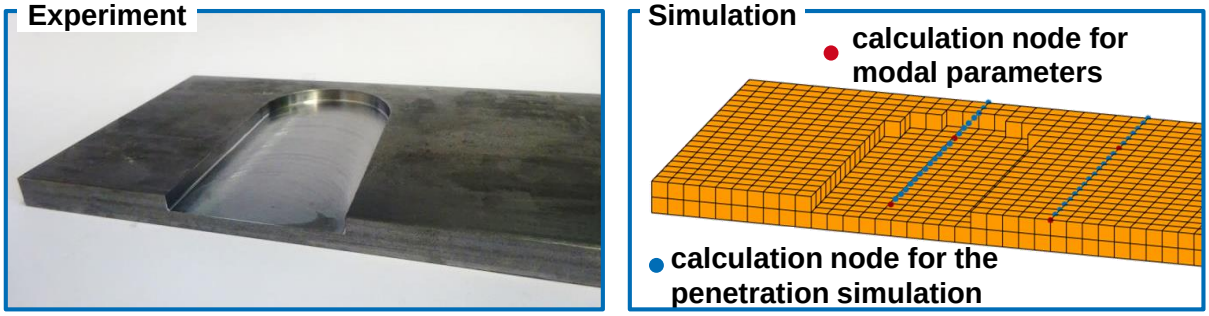

Figure 6. FE model of a workpiece after penetration simulation

(Voxel representation). Since the node coordinates and element arrays of the cubic elements are available in the FE Model, a Voxel representation is most convenient. This is used for a 2.5 dimension tool-workpiece penetration simulation. For each sampling point, the penetration simulation decides which elements are penetrated by the milling cutter. There are three possible cases for this decision. Either an element is fully penetrated, partly penetrated or not penetrated at all. The first case results in the removal of the element, the last case doesnot. The second case needs a more complex decision. As the depth of cut is a multiple of the edge length of an element, the partial penetration can be approximated by a two dimensional geometric penetration as both bodies have a full penetration in the third dimension. The criteria for the removal of a partly penetrated element is that 50% of its volume or more is penetrated. As the milling cutter has a much bigger diameter than the length of one element, the penetration is simplified by a direct connection of the two points of intersectionof the tool with the element. If the center of an element is part of the two dimensional trapezoid form, the trapezoid takes up at least 50% of the area of the full square. In this case the finite element is removed, otherwise the element remains. This simplifies the calculation of the penetrated area to detect whether the cubic center lies within the trapezoid or not. However, the overlapping form, comprises of a trapezoid and a circle segment, is ignored for simplicity. The effect of the error due to the trapezoidal simplification for two extreme cases is depicted in. Here, $'p'$ corresponds to the ratio of cutter diameter (D_F)to the element edge length (l_{El}). This error tends to a very small value for large diameters tools with fine meshes. For the current paper, a $'p'$ value of five was used which corresponds to an error between 4 to 5 %, which is found to be acceptable for the penetration simulation.

An example of the above described penetration simulation for a real workpiece is shown in Figure 6. The removal of individual elements from the raw workpiece model is achieved by the method of substructure decoupling.

The modal parameters of the workpiece are then calculated at each of the calculation nodes (red dots).

3. SUBSTRUCTURE DECOUPLING OF FINITE ELEMENTS

A prerequisite for performing substructure decoupling in the physical domain is the availability of the discretized structure to be subtracted and the discretized subtracting structure (in our case, a single cubic element). Both component files have to contain the following properties: The mass matrix M, the stiffness matrix K, a vector of degrees of freedom, a list of nodes, a vector of coordinates of the nodes in the domain and an element array that concludes which nodes build a hexahedron. The result of the penetration simulation provides the necessary information of both these discretized structures. Thus, an iterative decoupling can be carried out in order to get the various states of machining of the workpiece.

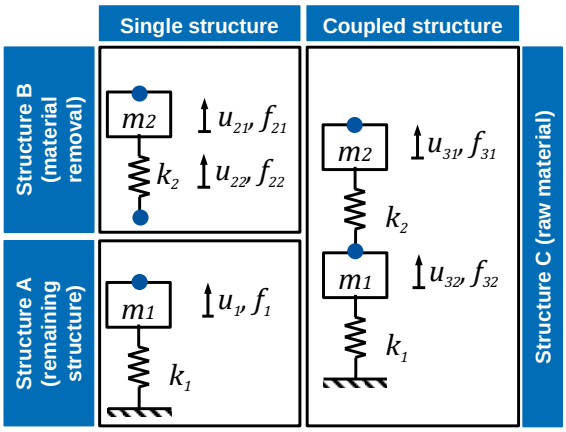

Figure 7. Analytical discreet mass system for decoupling

The decoupling approach in physical domain is illustrated here using a simple example of a system with two discrete masses and corresponding stiffness based on [KLER 2008]. The coupled structure, representing the raw workpiece is represented by Structure C (Fig.7). The subtracting structure is represented by Structure B and remaining structure (machined workpiece) by Structure A. Ultimately, the M, K matrices and the node information of Structure A must be determined. For the considered system, structure B is subtracted from structure C, resulting in structure A. In other words, B will be added to C with a negative sign, which results in B being removed from the total structure. The mathematical formulation for decoupling is described briefly in the following, where the matrix $\mathbf{M}$ is the mass matrix, matrix $\mathbf{K}$ is the stiffness matrix, vector $\mathbf{f}$ is the force vector, vector $\mathbf{u}$ is the displacement vector and vector $\ddot{\mathbf{u}}$ is the acceleration vector. The superscripts A, B, and C correspond to the respective structures.

Properties of Structure C:

$$\mathbf{M}^C=\begin{bmatrix} m_1 & 0 \\ 0 & m_2 \end{bmatrix},\ \mathbf{K}^C=\begin{bmatrix} k_1+k_2 & -k_2 \\ -k_2 & k_2 \end{bmatrix},\ \mathbf{f}^C=\begin{bmatrix} f_1^C \\ f_2^C \end{bmatrix},$$

$$\mathbf{u}^C=\begin{bmatrix} u_1^C \\ u_2^C \end{bmatrix} \text{ and } \ddot{\mathbf{u}}^C=\begin{bmatrix} \ddot{u}_1^C \\ \ddot{u}_2^C \end{bmatrix}$$

Properties of Structure B:

$$\mathbf{M}^B=\begin{bmatrix} m_2 & 0 \\ 0 & 0 \end{bmatrix},\ \mathbf{K}^B=\begin{bmatrix} k_2 & -k_2 \\ -k_2 & k_2 \end{bmatrix},\ \mathbf{f}^B=\begin{bmatrix} f_1^B \\ f_2^B \end{bmatrix},$$

$$\mathbf{u}^B=\begin{bmatrix} u_1^B \\ u_2^B \end{bmatrix} \text{ and } \ddot{\mathbf{u}}^B=\begin{bmatrix} \ddot{u}_1^B \\ \ddot{u}_2^B \end{bmatrix}$$

Subtraction of Structure B from C gives:

$$\mathbf{M}=\begin{bmatrix} m_1 & 0 & 0 & 0 \\ 0 & m_2 & 0 & 0 \\ 0 & 0 & -m_2 & 0 \\ 0 & 0 & 0 & 0 \end{bmatrix},$$

$$\mathbf{K}=\begin{bmatrix} k_1+k_2 & -k_2 & 0 & 0 \\ -k_2 & k_2 & 0 & 0 \\ 0 & 0 & -k_2 & k_2 \\ 0 & 0 & k_2 & -k_2 \end{bmatrix},\ \mathbf{u}=\begin{bmatrix} u_1^C \\ u_2^C \\ u_1^B \\ u_2^B \end{bmatrix},\ \ddot{\mathbf{u}}=\begin{bmatrix} \ddot{u}_1^C \\ \ddot{u}_2^C \\ \ddot{u}_1^B \\ \ddot{u}_2^B \end{bmatrix}$$

$$\text{and } \mathbf{f}=\begin{bmatrix} f_1^C \\ f_2^C \\ -f_1^B \\ -f_2^B \end{bmatrix}$$

With,

$$\mathbf{Bu}=\begin{bmatrix} B_1 & B_2 & B_3 & B_4 \end{bmatrix}\begin{bmatrix} u_1^C \\ u_2^C \\ u_1^B=u_2^C \\ u_2^B=u_1^C \end{bmatrix}=0 \Leftrightarrow \mathbf{B}=\begin{bmatrix} 1 & 0 & 0 & -1 \\ 0 & 1 & -1 & 0 \end{bmatrix} \quad (1)$$

where B is a signed Boolean matrix that operates on the interface DOF and u is a vector of all DOFs. Furthermore,

$$\mathbf{Lq}=\mathbf{u} \Leftrightarrow \begin{bmatrix} 1 & 0 \\ 0 & 1 \\ 0 & 1 \\ 1 & 0 \end{bmatrix}\begin{bmatrix} u_1^C \\ u_2^C \end{bmatrix}=\begin{bmatrix} u_1^C \\ u_2^C \\ u_1^B \\ u_2^B \end{bmatrix} \quad (2)$$

$$\text{with } \mathbf{L}=\begin{bmatrix} 1 & 0 \\ 0 & 1 \\ 0 & 1 \\ 1 & 0 \end{bmatrix} \text{ and } \mathbf{q}=\begin{bmatrix} u_1^C \\ u_2^C \end{bmatrix}$$

where L is a Boolean matrix localizing the interface DOF and q is the unique set of interface DOF for the system. The decoupled system (Structure A) can then be derived by,

$$\tilde{\mathbf{M}}=\mathbf{L}^T\mathbf{M}\mathbf{L}=\begin{bmatrix} 1 & 0 & 0 & 1 \\ 0 & 1 & 1 & 0 \end{bmatrix}\begin{bmatrix} m_1 & 0 & 0 & 0 \\ 0 & m_2 & 0 & 0 \\ 0 & 0 & -m_2 & 0 \\ 0 & 0 & 0 & 0 \end{bmatrix}\begin{bmatrix} 1 & 0 \\ 0 & 1 \\ 0 & 1 \\ 1 & 0 \end{bmatrix}=\begin{bmatrix} m_1 & 0 \\ 0 & 0 \end{bmatrix}=\mathbf{M}^A \quad (3)$$

$$\tilde{\mathbf{K}}=\mathbf{L}^T\mathbf{K}\mathbf{L}=\begin{bmatrix} 1 & 0 & 0 & 1 \\ 0 & 1 & 1 & 0 \end{bmatrix}\begin{bmatrix} k_1+k_2 & -k_2 & 0 & 0 \\ -k_2 & k_2 & 0 & 0 \\ 0 & 0 & -k_2 & k_2 \\ 0 & 0 & k_2 & -k_2 \end{bmatrix}\begin{bmatrix} 1 & 0 \\ 0 & 1 \\ 0 & 1 \\ 1 & 0 \end{bmatrix}=\begin{bmatrix} k_1 & 0 \\ 0 & 0 \end{bmatrix}=\mathbf{K}^A \quad (4)$$

$$\tilde{\mathbf{f}}=\mathbf{L}^T\mathbf{f}=\begin{bmatrix} 1 & 0 & 0 & 1 \\ 0 & 1 & 1 & 0 \end{bmatrix}\begin{bmatrix} f_1^C \\ f_2^C \\ -f_1^B \\ -f_2^B \end{bmatrix}=\begin{bmatrix} f_1^A \\ 0 \end{bmatrix}=\mathbf{f}^A \quad (5)$$

In this way, an FE model with the corresponding M and K matrices of the machined workpiece can be obtained. This can subsequently be used for the calculation of modal parameters of the workpiece.

4. EXPERIMENT AND RESULTS

In this chapter, a validation of the developed method is carried out. A specimen workpiece made of medium carbon steel (C45) with a bridge in the middle is selected in order to enable a significant change in workpiece dynamics due to reduction in volume. It is fixed to the machine table using four M12 bolt connections. The machine used is a mid-sized 3-axis milling center. The FE model of the raw workpiece with the different intermediate machining is shown in Figure 8. The workpiece is cut in nine intermediate steps. The stiffness

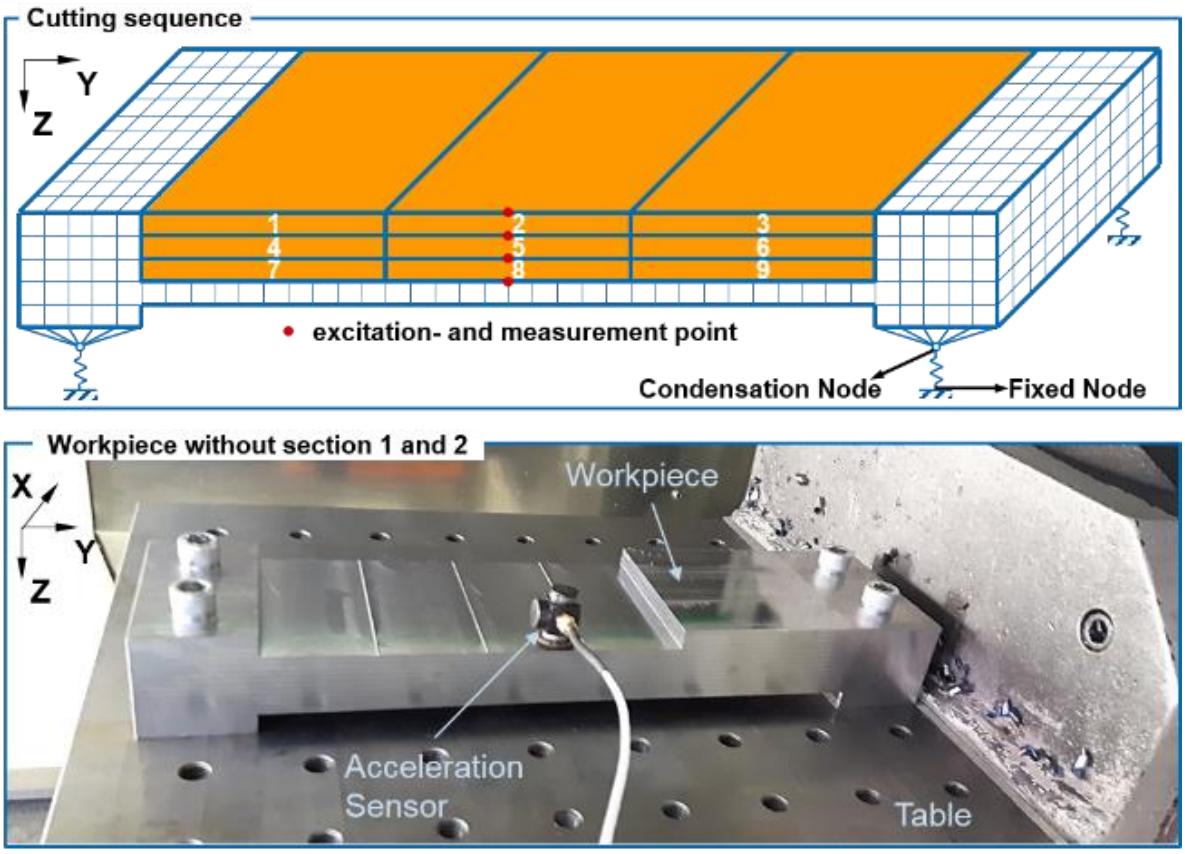

Figure 8. Simulated workpiece at different stages of material removal (top) and measurement setup for a machining state (below)

of the machine is represented by four spring elements connected between a condensation node and a fixed node.

For the described workpiece and its intermediate states the direct FRFs are measured at the highest point in the middle of the 'bridge' at one edge in the z direction (red dots in Figure 8) after the W/P was fixed to the M/C table. Additionally, a experimental modal analysis was conducted for every intermediate machining state of the workpiece. These measurements serve as the validation for simulated FRFs of the modelled workpiece-machine system. Also, the experimental modal analysis allows the validation of the simulated mode shapes of the workpiece.

A state space Eigenvalue problem is solved for the M, K and C matrices obtained from the decoupling step using an assumed modal damping ratio of 0.001 for the damping matrix C. Only the first ten eigenvalues are calculated in order to reduce computational time. Subsequently, a driving point FRF is calculated for the workpiece at the corresponding point on the bridge (red dots in Figure 8). The measured and simulated FRFs for different intermediate states are illustrated in Fig. 9 a) and a comparison of a few states is shown in Figure 9 b).

With an increase in volume of removed material, the workpiece becomes more compliant, as shown in Fig. 9 a). Due to the loss of mass and stiffness, the direct FRF at the center of the bridge of the workpiece shows a shifting of the dynamics towards the lower frequencies and the increase in the static compliance. Comparisons of the FRFs at a particular state of material removal are made in Fig. 9 b). The measured and simulated FRFs correspond very well in the observed frequency range and in the static compliance. The first two dominant resonance peaks of the workpiece corresponding to the first bending mode and first torsion mode of the bridge could be predicted reasonably well for all states of the workpiece. The resonance peak at around 2000 Hz in the FRF for raw workpiece and for 33 % machined part could not be identified in the simulated FRF. The experimental modal analysis shows that this resonance corresponds to a vibration mode of the machine. Since in this paper the machine stiffness is only represented by four spring elements, this resonance could not be depicted in the simulation.

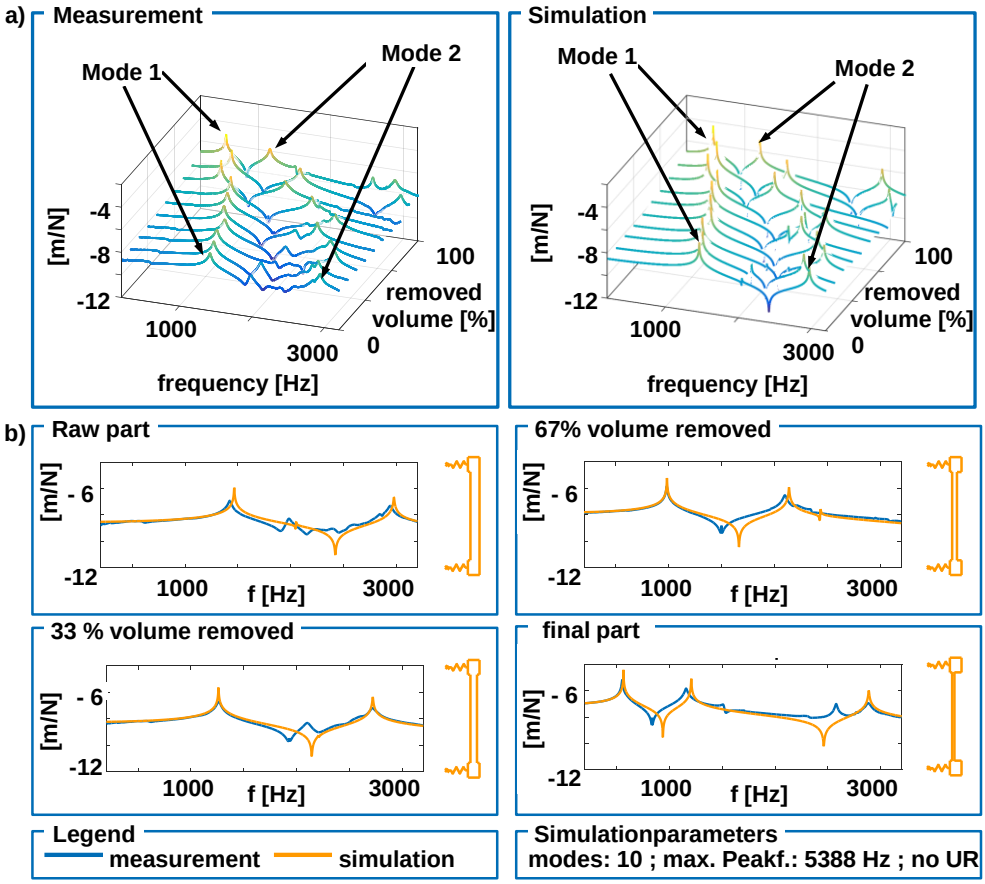

Figure 9. Measured and predicted direct compliances of the workpiece

Although the resonance frequencies or poles could be predicted well, the anti-resonances could not be accurately predicted. This is possibly due to the modal truncation and ignoring of the upper residues [Avitabile 2002].

5. CONCLUSIONS

The current paper proposes a method considering the influence of workpiece dynamics at different stages of material removal. In this approach, the workpiece is discretized with cubic elements and represented as a voxel model for the subsequent penetration simulation. Using the penetration simulation, the modal parameters of different states of material removal could be calculated. The simulated FRFs at each state of the workpiece were coupled with spring elements to represent the machine stiffness. In future work, the frequency response at the workpiece coupling points could be coupled with the measured machine dynamics to account for both, static and dynamic behavior of the machine. Additionally, a method for reducing the workpiece model without compromising on the accuracy of the penetration simulation would be needed in order to reduce computational time.

ACKNOWLEDGEMENTS

The authors wish to gratefully acknowledge the support of the German Research Foundation (Deutsche Forschungsgemeinschaft, DFG). This work was funded as part of the DFG Project ''Experimental substructure coupling for vibration analysis in machine tools'' (Project Number- BR 2905/55-2).

REFERENCES

[Altinas 2014] Altinas, Y., Kersting, P., Biermann, D., Budak, E., Denkena, B., Lazoglu, I. Virtual process systems for part machining operations. In: CIRP Annals - Manufacturing Technology. 63(2), 2014, pp. 585-605 [DOI: https://doi.org/10.1016/j.cirp.2014.05.007]

[Avitabile 2002] Avitabile, P. Twenty years of structural dynamic modification – A review. In: Journal of Sound and Vibration, 37 (1), 2003, pp. 14-27

[Brecher 2015] Brecher, C., Fey, M., Tenbrock, C., Daniels, M. Multipoint Constraints for Modeling of Machine Tool Dynamics. In: Journal of Manufacturing Science and Engineering. 138, 2015 [DOI: 10.1115/1.4031771]

[Brecher 2016] Brecher, C., Fey, M., Daniels, M. Modeling of Position-, Tool- and Workpiece-Dependent

Milling Machine Dynamics. In: High Speed Machining, 2016 [DOI: https://doi.org/10.1515/hsm-2016-0002]

[De Klerk 2008] de Klerk, D., Rixen, D. J., Vormeeren, S. N.: General framework for dynamic substructuring history review and classification of techniques. In: AIAA Journal Vol. 46, No. 5, 2008, pp. 1169-1181.

[Law 2013] Law, M., Phani, A. S. Altintas, Y. Position-dependent multibody dynamic modeling of machine tools based on improved reduced order models. In: Journal of Manufacturing Science and Engineering. 135(2)

[Law 2014] Law, M., Rentzsch, H., Ihlenfeldt, S. Evaluating mobile machine tool dynamics by substructure synthesis. In: Advanced Materials Research. 1018, 2014, pp.

[Liu 2011] Liu, H., Zhao, W., Zhang, J., Wang, L., Ma, X., Zhao, F. Modal analysis of machine tools during working process by matrix perturbation method. In: Assembly and Manufacturing (ISAM), 2011 [DOI: 10.1109/ISAM.2011.5942321]

[Liu 2014] Liu, H., Wang, L., Zhao, W. Analysis of position-dependent dynamic characteristics for machine tools using a variable-coefficient linear model. In: Journal of Mechanical Engineering Science. 228(15), 2014, pp. 2690-2701

[Tuysuz 2017] Tuysuz, O., Altintas, Y. Frequency Domain Updating of Thin-Walled Workpiece Dynamics Using Reduced Order Substructuring Method in Machining. In: Journal of Manufacturing Science and Engineering. 139(7), 2017, pp. 071013

[Weck 2006] Weck, M., Brecher, C. Werkzeugmaschinen – Band 5. (Series: Werkzeugmaschinen. Bd. 5). 7th ed., 2006. ISBN 978-3-540-32951-0

[Yang 2016] Yang, Y., Zhang, W. H., Ma, Y. C., Wan, M. Chatter prediction for the peripheral milling of thin-walled workpieces with curved surfaces. In: International Journal of Machine Tools and Manufacture. 109, 2016, pp. 36-48

[Yigit 2002] Yigit, A. S., Ulsoy, A. G., Allahverdi, A. Optimizing modular product design for reconfigurable manufacturing. In: Journal of Intelligent Manufacturing. 13(4), 2002, pp. 309-316

CONTACT:

Prateek Chavan M.Sc.
WZL RWTH Aachen
Steinbachstrasse 19, Aachen, 52074, Germany
e-mail: P.Chavan@wzl.rwth-aachen.de